



Behavior of Sand Specimens Subjected to Cyclic Loads under Drained and Undrained Conditions in Variable Loading Amplitudes

Van Thuy Do¹⁾, Van Hieu Nguyen¹⁾*, Duc Tiep Pham¹⁾

¹⁾ Institute of Technology for Special Engineering, Le Quy Don Technical University, Hanoi, Vietnam.

* Corresponding Author. E-Mails: thuydv@qdtu.edu.vn; dovanthuyhvkts@gmail.com

ARTICLE INFO

Article History:

Received: 18/7/2023

Accepted: 10/3/2024

ABSTRACT

Dynamic loads with different magnitudes cause shear stress and strain in the soil and increase the pore water pressure, reducing soil strength and leading to structural failure. This article presents the behavior of natural river-sand specimens subjected to cyclic loads under both drained and undrained conditions, as observed in cyclic triaxial tests conducted in the laboratory. The experiments were performed on sand specimens with a relative compaction of 0.95 when changing the loading amplitude with three different levels of 30 kPa, 50 kPa and 60 kPa. Experimental results show that, under the condition of drained cycle load, the pore water pressure does not form; only accumulated strain and dynamic parameters are almost unchanged. Meanwhile, with the condition of undrained cyclic load, the pore water pressure increases and causes liquefaction of the specimen, then the axial strain increases dramatically and is not capable of recovery. When varying the loading amplitude under drained condition, the initial-strength values increase as the amplitude of the load increases. This trend has the opposite direction when testing under undrained condition, which means that when increasing the loading amplitude, the initial-strength values decrease and the liquefaction potential of the specimens is faster. Further, under the undrained condition, the loading amplitude of 30 kPa effect is almost negligible on the liquefaction ability of the specimen.

Keywords: Sand, Drained condition, Undrained condition, Loading amplitude, Cyclic triaxial tests.

INTRODUCTION

The behavior of soil specimens subjected to cyclic loads in drained and undrained conditions is an important area of study in geo-technical engineering (Vedran Jagodnik and Željko Arbanas, 2022). These studies aimed to understand how soil responds and deforms under cyclic loading and unloading when the drained conditions vary (Souza Junior et al., 2020). By

investigating this behavior, engineers can better predict the performance of soil in various geo-technical applications, such as foundation design, slope-stability analysis and offshore structures.

In drained condition, the soil specimens are allowed to freely drain excess pore water pressure generated during loading and unloading cycles. This condition mimics scenarios where the soil is well-drained, such as sands or cohesionless soils with adequate permeability.

Under cyclic loads, the soil experiences changes in stress and strain, leading to various responses. These can include progressive accumulation of deformation, such as shear strain, axial strain, dilation and settlement (Wichtmann et al., 2005). The drained behavior of soil specimens can be influenced by factors, such as confining pressure, stress history and the initial void ratio of the soil (Duque et al., 2022).

On the other hand, undrained condition occurs when the soil specimens are not allowed to drain during cyclic load. This situation represents cases when the load has affected in a short time, which causes inadequate drainage in the specimen, or when the drained condition of the soil is not guaranteed. In undrained condition, the excess pore water pressure generated during loading is not dissipated and can significantly affect soil behavior. The undrained response of sand specimens can exhibit phenomena, like pore pressure buildup, contractive or dilative behavior and potential liquefaction under certain loading conditions (Zhehao Zhu et al., 2021). The undrained shear strength and stress-strain behavior of the soil are crucial factors in assessing stability and the potential for catastrophic failure in geo-technical structures.

Studying the behavior of sand specimens under cyclic loads in both drained and undrained conditions helps engineers gain insights into the soil's response and its influence on geo-technical applications. This knowledge aids in the design of foundations, retaining structures and earthworks, as well as in evaluating the

stability and performance of natural and engineered slopes. Furthermore, understanding the cyclic behavior of sand in drained and undrained conditions is vital for mitigating geo-technical hazards and ensuring the safety and reliability of infrastructure projects in various geological settings.

In this research, the behavior of river-sand specimens with a relative compaction of 0.95 is studied under drained and undrained cyclic loads in the laboratory with the change of three different loading amplitudes of 30 kPa, 50 kPa and 60 kPa in over 5000 loading cycles, which is a long enough time to evaluate the effect of a type of dynamic load, such as an earthquake which takes only a few minutes. This study provides significant insights into soil behavior, which is crucial for the design of foundations and other geo-technical structures.

MATERIALS AND METHODS

Experimental Materials and Specimen Reconstitution

Uniform and clean sand (grain diameter from 0.1 to 1.0 mm) has been used in this study, which was taken from the Trai Giam mine in Ham Tan district in Binh Thuan province in Vietnam. This sand is analyzed through grain size (Figure 1), relative compaction testing and specific gravity testing, as illustrated by the parameters in Table 1.

The grain-size curve of sand is presented in Figure 1 (ASTM D422-63).

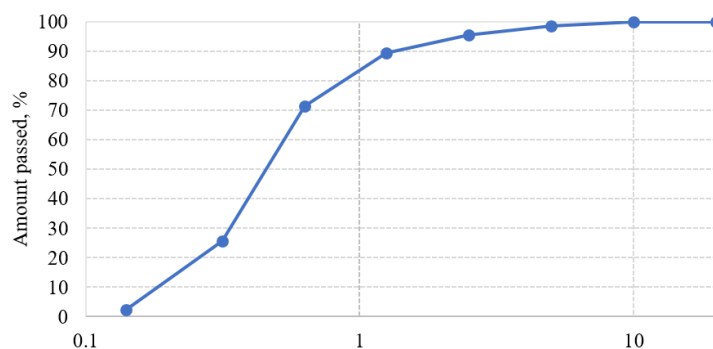


Figure (1): Grain-size curve of the experimental sand

The sand is reconstituted to achieve a relative compaction (K) of 0.95. The relative compaction referred to here is the ratio of the dry soil under compaction to the maximum dry unit weight of the soil obtained during the laboratory compaction test (ASTM

D698-12 and Braja M. Das and Khaled Sobhan, 2013), which is determined by the formula:

$$K = \frac{\gamma_k}{\gamma_k^{max}} \quad (1)$$

where K is the required relative compaction (dimensionless), γ_k is the dry soil (kN/m^3) and γ_k^{max} is the maximum dry unit weight in the laboratory (kN/m^3).

To determine the value of maximum dry unit weight, the authors compacted the specimen with five different

moisture content levels (ASTM D1557-12 and Vietnamese standard 8721). From there, a relationship curve between dry soil and moisture content is presented in Figure 2.

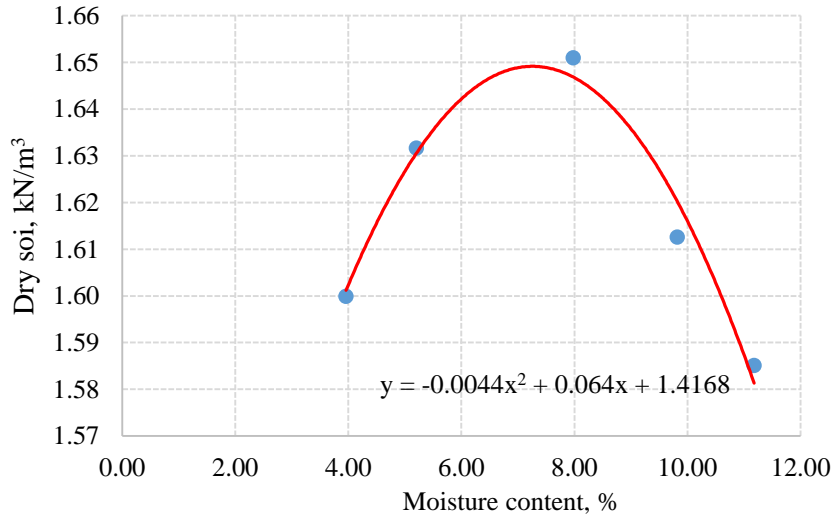


Figure (2): Relationship curve of compacted dry soil and moisture content of sand

From the function shown in Figure 2, the maximum dry unit weight γ_k^{max} is calculated as 1.65 g/cm^3 with an

optimum moisture content w_o of 7.27%.

Table 1. Typical parameters of sand used for the experiment

Characteristic	Symbol	Value	Unit
Specific gravity	G_s	2.64	-
Effective grain size	D_{10}	0.183	mm
Relative compaction	K	0.95	-
Maximum dry unit weight	γ_k^{max}	1.65	kN/m^3
Optimum moisture content	w_o	7.27	%

Methods

Theoretical Methods of Soil Behavior When Subjected to Cyclic Loads in Drained and Undrained Conditions

Method for Consolidated Drained Soil

In this test method, the shear characteristics are measured under drained condition and applied to field conditions where soils have been fully consolidated. The shear strength can be expressed in terms of effective stress, because a strain rate or load application rate slow enough to allow pore pressure dissipation during shear is used to result in negligible excess pore pressure conditions (ASTM D7181 - 20).

The axial strain is determined for a given applied

axial load as follows:

$$\epsilon_1 = \frac{\Delta H}{H_c}, \tag{2}$$

where ϵ_1 is the axial strain, ΔH is the change in the height of the specimen during loading (mm), H_c is the height of the specimen after consolidation (mm), which is determined from the following equation:

$$H_c = H_0 - \Delta H_0, \tag{3}$$

with H_0 being the initial height of the specimen (mm), while ΔH_0 being the change in height of the specimen at the end of consolidation (mm).

The principal stress difference (deviator stress), $\sigma_1 - \sigma_3$, for a given applied axial load is calculated as follows:

$$(\sigma_1 - \sigma_3) = \frac{P + K + \sigma_3 \cdot (A - a)}{A} - \sigma_3, \tag{4}$$

where A is the corresponding cross-sectional area (mm^2), a is the area of the loading piston at the point where it enters the cell (mm^2), σ_1 is the major principal stresses in a triaxial test (kPa), σ_3 is the minor principal stresses in a triaxial test (kPa), P is the load to be applied to the piston to reach σ'_{vc} (vertical effective stress), calculated as follows:

$$P = (\sigma'_{vc} - \sigma'_{hc}) \cdot A_c - K + (\sigma'_{hc} + u_b)a;$$

$$K = W - [(A_c - a) \cdot h_c \cdot \gamma], \quad (5)$$

with σ'_{vc} being the vertical effective stress, defined at the center of the specimen (kPa), σ'_{hc} the lateral effective stress, defined at the center of the specimen (kPa), A_c the area of the specimen after isotropic consolidation computed (mm^2), u_b the back pressure (kPa), h_c the distance from the top of loading cap to mid-height of the specimen, after isotropic consolidation (mm) and W is the weight of the piston, top cap and top half of specimen (g).

Method for Consolidated Undrained Soil

The constitutive relation of dynamic parameters is determined by the axial stress and strain in the specimen (ASTM - D3999).

The axial stress and strain in the specimen can be obtained from its response to increasing dynamic loading. The maximum dynamic shear stress τ_d and dynamic strain δ_d in the specimens are calculated according to the following equations:

$$\tau_d = \frac{\sigma_d}{2}; \quad (6)$$

$$\delta_d = (1 + \mu) \cdot \varepsilon_d, \quad (7)$$

where σ_d is the maximum dynamic stress in the specimen (kPa), ε_d is the maximum dynamic strain in the specimen (mm) and μ is the Poisson's coefficient of the material.

The dynamic elasticity modulus (Young's modulus) is determined from the behavior of soil through the stress-strain under cyclic axial load (Figure 3) and can be calculated as follows:

$$E_d = \frac{\sigma_d}{\varepsilon_d} = \frac{\frac{(\sigma_{d1} - \sigma_{d2})}{2}}{\frac{(\varepsilon_{d1} - \varepsilon_{d2})}{2}}, \quad (8)$$

where σ_{d1} , σ_{d2} , ε_{d1} , and ε_{d2} are the maximum values

of axial compressive stress, axial tensile stress, axial compressive strain and axial tensile strain, respectively.

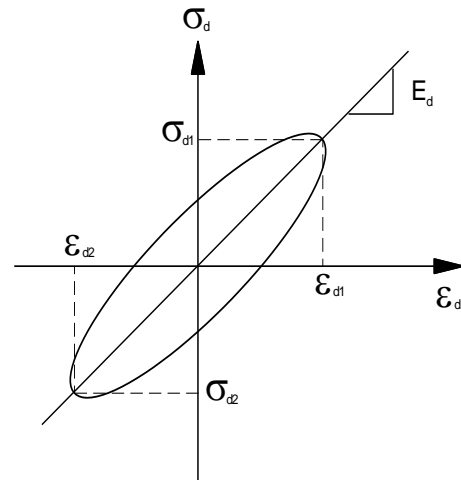


Figure (3): Stress-strain behavior of soil under cyclic load and determination of elasticity modulus

Therefore, the dynamic shear modulus of a specimen is defined as:

$$G_d = \frac{E_d}{2 \cdot (1 + \mu)}. \quad (9)$$

The damping ratio is an important dynamic parameter of soil that expresses the hysteresis characteristic of its stress-strain behavior under cyclic loading (Figure 4), which is determined as follows (Jianfeng Li et al., 2020):

$$D = \frac{A_L}{4 \cdot \pi \cdot A_T} \cdot 100\%, \quad (10)$$

where A_L is the area inside the hysteresis loop (kN-m), A_T is the area of the triangle calculated and $A_T = 0.5 \cdot L \cdot S$, with L and S being the edges joined by the hysteresis loop and the coordinate axes (Figure 4).

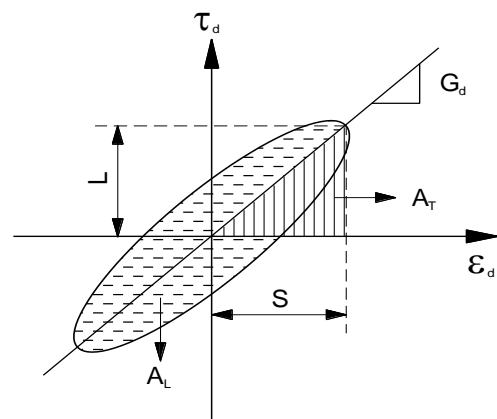


Figure (4): Determining the shear modulus and damping ratio of soil under cyclic load

Experimental Method for Sand Specimens Subjected to Cyclic Loads in Drained and Undrained Conditions

The experiments in this study were performed on a cyclic triaxial apparatus (Figure 6). The test specimens are compacted in a circular cylindrical mold with a diameter of 7 cm and a height of 14 cm (Md Asfaque Ansari and Lal Bahadur Roy, 2023). When compacting each layer in the mold, it is necessary to control the uniformity of calculated relative compaction.

The experimental stages were performed as follows:

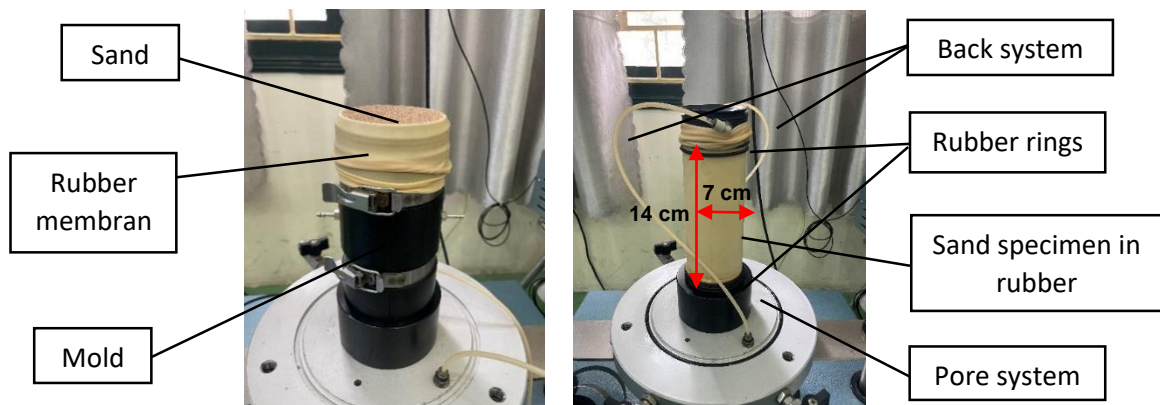


Figure (5): Reconstituted-specimen preparation by compaction method

Natural-saturation Stage

Put the specimen under vacuum before removing the prototyping mold. Place the triaxial cell and let the degassed water from the tank enter it. The initial pressure has been created in the triaxial cell to stabilize the specimen when it is no longer under vacuum. Aerate the carbon dioxide through the specimen by the pore and

Reconstituting-specimen Stage

The soil mass and the amount of water to create moisture for the specimen are calculated with the studied relative compaction. The rubber membrane is placed on the specimen mold. Rubber rings are used to seal the bottom and top of the specimen. The specimen is compacted into the mold and a reconstituted specimen is obtained with a diameter of 7 cm and a height of 14cm, as shown in Figure 5. The specimens must be absolutely sealed.

back systems for 30 to 40 minutes to push out all other gases in the specimen (Figure 6a). Next, natural saturation is achieved by passing degassed water through the specimen through the pore and back systems. The water will dissolve the carbon dioxide present in the specimen and fill the voids with water (Figure 6b).

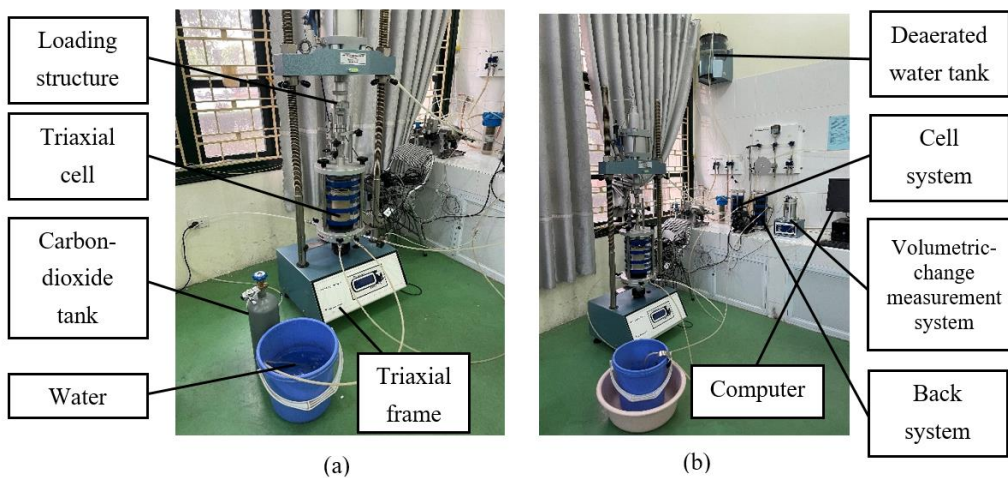


Figure (6): Naturally-saturated specimen with carbon dioxide and degassed water

Saturation Stage by Device: Start equipment, such as aircompressor, gauge device and computer. Increase the value of the cell back pressure until the saturation value $B \geq 0.95$ is obtained (displayed on the computer). Save the back-pressure value at the time of saturation.

Consolidation Stage by Device: Set the back-pressure target to the value at the previous saturation step. The cell-pressure target value equals the back value plus 100 kPa. Perform specimen consolidation until the consolidation degree reaches over 98% and the effective stress of 100 kPa, then stop.

Stage of Performing the Load: Set parameters on Dyna Triaxial software, such as undrained or drained condition, loading type, loading frequency, effective pressure, loading amplitude and number of observation cycles. In this study, the load is axial and sinusoidal with the frequency of 0.5 Hz (ASTM-D3999). The loading amplitude is calculated by the formula:

$$A_{Load} = 2 \cdot CSR \cdot \sigma'_0 \quad (11)$$

where A_{Load} is the loading amplitude (kPa) and CSR is the stress ratio, which is between 0.15 and 0.3 (ASTM-D3999), σ'_0 is the effective stress (kPa), in this research $\sigma'_0 = 100 \text{ kPa}$. The authors used three different CSR values of 0.15, 0.25 and 0.3. Therefore, the specimens have been subjected to cyclic loads of varying amplitudes (30 kPa, 50 kPa and 60 kPa) and their behaviors have been closely monitored.

Next, observe the experiment through the number of loading cycles (T.S. Hou et al., 2020).

RESULTS AND DISCUSSION

Results

Behavior of Sand Subjected to Cyclic Load in Drained Condition

Under the effect of cyclic load in drained condition with thousands or even millions of loading cycles, the test specimens only have strain accumulation. Therefore, in this study, the authors observe the behavior of sand specimens under drained condition with over 5000 cycles. It can be seen that the strain of the sand specimens only increases slowly and moderately. It seems that the grains are arranged more stable and dynamic parameters such as axial strain, damping ratio and Young's modulus change very little and tend to be steady.

In the cyclic load under drained condition, the results indicate that the axial strain is cumulative from 0.02 to 0.03 at the loading amplitude of 30 kPa. This value changes from 0.03 to 0.05 at the loading amplitude of 50 kPa and from 0.03 to 0.06 at the loading amplitude of 60 kPa (Figure 7).

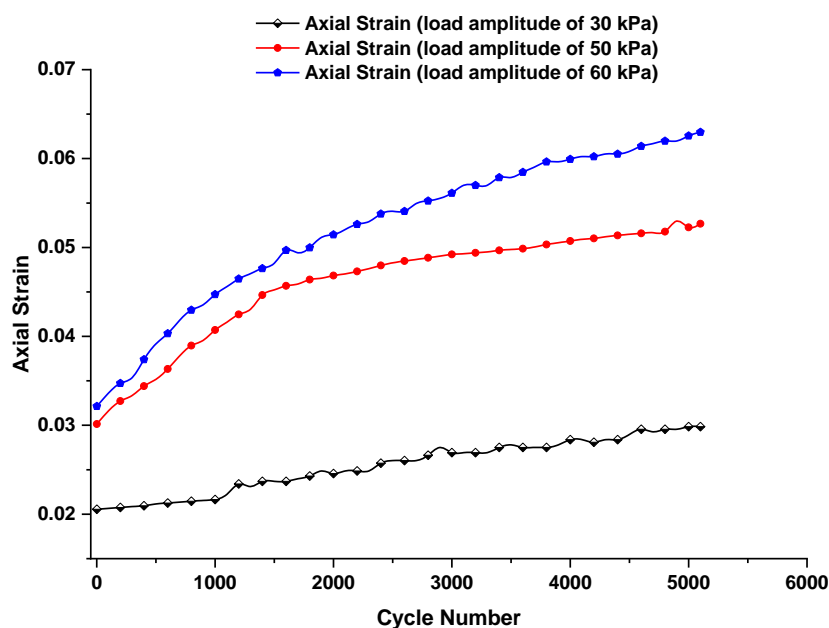


Figure (7): Axial-strain accumulation of sand specimens subjected to cyclic load in drained condition with varying loading amplitudes

Considering the damping ratio of the specimens when changing the amplitude of cyclic load applied in drained condition, with the loading amplitude of 60 kPa, the damping ratio has a higher value, with a stability of

between 5.5% and 5.8%. In the two remaining cases of loading amplitude of 30 kPa and 50 kPa, the damping ratio has relatively equal values and the stability is between 4.3% and 4.7% (Figure 8).

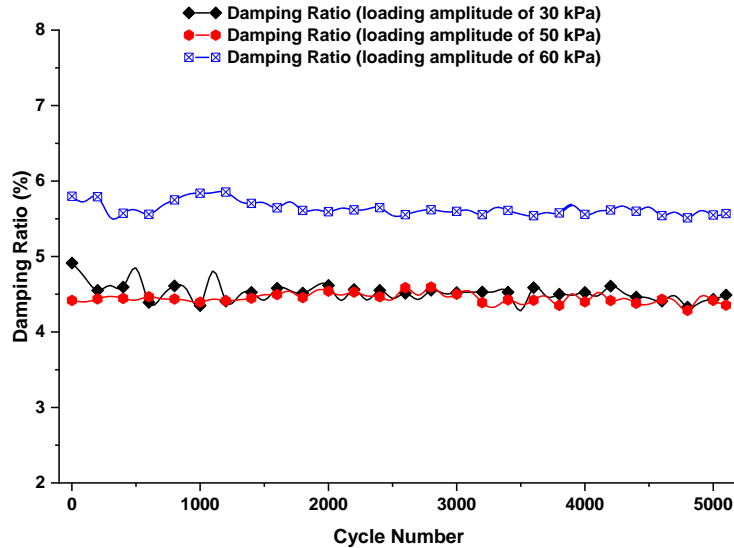


Figure (8): Damping ratio of sand specimens subjected to cyclic load in drained condition with varying loading amplitudes

Besides, it can be seen that the difference in Young's-modulus values with cases of loading changes in comparison with the damping ratio. With the loading amplitude of 30 kPa, Young's-modulus value is lower and the stability is between 100 MPa and 102 MPa.

Meanwhile, Young's-modulus value is stable between 146 MPa and 149 MPa with the loading amplitude of 50 kPa and between 149 MPa and 150 MPa with the loading amplitude of 60 kPa (Figure 9).

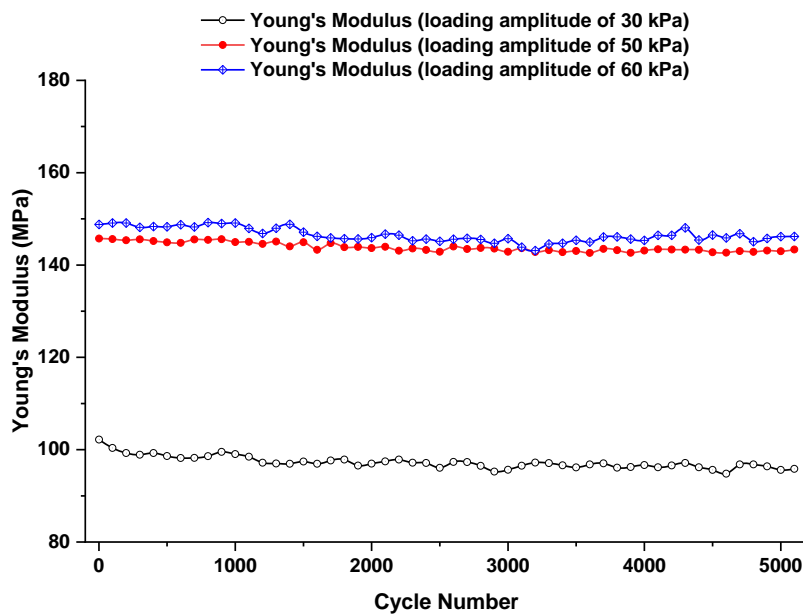


Figure (9): Young's modulus of sand specimens subjected to cyclic load in drained condition with varying loading amplitudes

Behavior of Sand Subjected to Cyclic Load in Undrained Condition

When the applied load is small with an amplitude of 30 kPa (corresponding to CSR_{min}), similar to the above case with over 5000 observation cycles, the specimen is almost only moderately deformed and the sand grains seem to be rearranged more stable. The sand specimen has not undergone the liquefaction phenomenon. The specimen is liquefied with a finite number of liquefaction cycles under the increase of loading amplitude. The liquefaction cycle number of the sand specimen is 1738 cycles at the loading amplitude of 50 kPa and 773 cycles at the loading amplitude of 60 kPa.

It can be seen that the axial strain is cumulative from 0.02 to 0.03 at the loading amplitude of 30 kPa. Meanwhile, the rapid and unrecoverable rise of the axial strain has been seen in the remaining loading- amplitude cases (Figure 10).

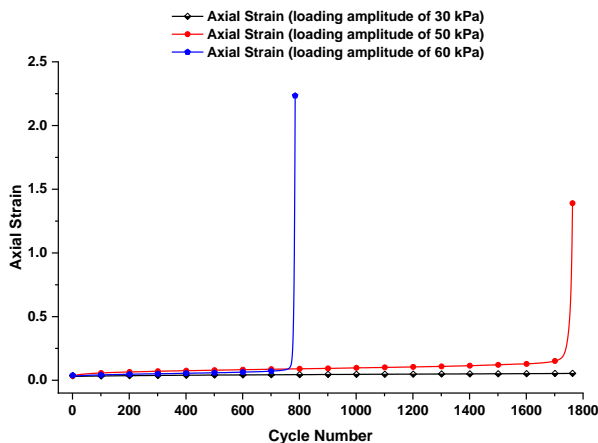


Figure (10): Axial-strain accumulation of sand specimens subjected to cyclic load in undrained condition with varying loading amplitudes

Considering the damping ratio of the specimens when changing the amplitude of cyclic loads applied in undrained condition, with the loading amplitude of 30 kPa, the damping ratio is stable between 1.1% and 1.5%. The sand specimen has an increase of the damping ratio from 4.2% to 17% at the loading amplitude of 50 kPa and from 5% to 19% at the loading amplitude of 60 kPa when the specimens have been liquefied (Figure 11).

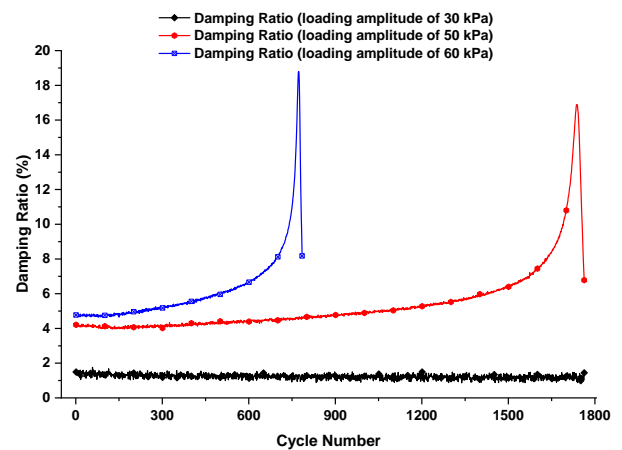


Figure (11): Damping ratio of sand specimens subjected to cyclic load in undrained condition with varying loading amplitudes

Meanwhile, a decrease of Young's modulus from 189 MPa to about 173 MPa is noticed, then it tends to stabilize at the loading amplitude of 30 kPa. We see a different trend in Young's modulus in the remaining loading-amplitude cases; its value decreases from 172 MPa at the loading amplitude of 50 kPa and from 167 MPa at the loading amplitude of 60 kPa, with a rapid-drop tendency at the time of liquefied specimen (Figure 12).

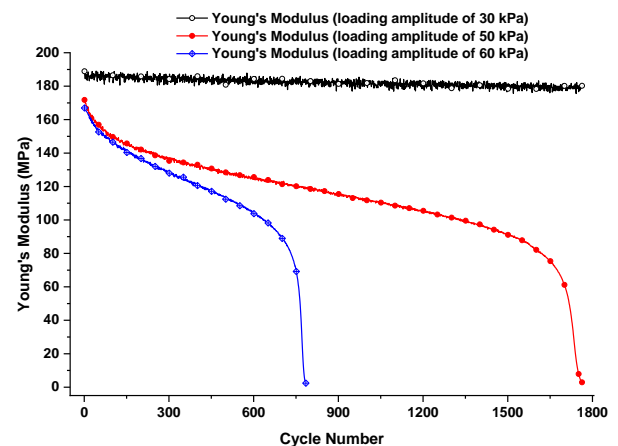


Figure (12): Young's modulus of sand specimens subjected to cyclic load in undrained condition with varying loading amplitudes

Comparison of Dynamic Parameters under Experimental Conditions

From the studied results, the authors built a table comparing the dynamic parameters studied for three loading magnitudes corresponding to three loading

amplitudes in drained and undrained conditions (Table 2).

Table 2. Dynamic parameters under loading in drained and undrained conditions

Values of research parameters	Loading amplitude (kPa)					
	Drained condition			Undrained condition		
	30 kPa	50 kPa	60 kPa	30 kPa	50 kPa	60 kPa
Number of observation cycles	Over 5000 cycles	Over 5000 cycles	Over 5000 cycles	Over 5000 cycles	Liquefied specimen with 1738 cycles	Liquefied specimen with 773 cycles
Axial strain	Accumulates from 0.02 to 0.03	Accumulates from 0.03 to 0.05	Accumulates from 0.03 to 0.06	Accumulates from 0.02 to 0.03	Increases very quickly when the specimen liquefies	Increases very quickly when the specimen liquefies
Damping ratio (%)	Stability between 4.3% and 4.5%	Stability between 4.5% and 4.7%	Stability between 5.5% and 5.8%	Stability between 1.1% and 1.5%	Increase from 4.2 % to 17 %	Increase from 5 % to 19 %
Young's modulus (MPa)	Stability between 100MPa and 102 MPa	Stability between 146MPa and 149 MPa	Stability between 149MPa and 150 MPa	Moderate decline from 189 MPa to 173 MPa	Decrease from 172MPa to very low	Decrease from 167MPa to very low

DISCUSSION

The results show that the sand behavior under cyclic loading varies significantly with the loading conditions, demonstrating its complexity.

The damping ratio has been observed in both drained and undrained conditions by cyclic triaxial tests (Figures 8 and 11). The damping ratio in these results is consistent with previous studies (Vedran Jagodnik and Željko Arbanas, 2022). Besides, it is worth noting that the damping-ratio values in this study are lower than the results of Vedran Jagodnik and Željko Arbanas (2022). Further, with a low loading amplitude of 30 kPa, despite loading in undrained condition, the sand specimen still tends to be stable, with rearrangement of particles and increase of compaction without causing liquefaction.

When the sand specimens are subjected to cyclic load under drained condition, the Young's-modulus value is significantly lower at the loading amplitude of 30 kPa, which is only 0.67 times that of the 60-kPa case.

The influence of loading amplitude under undrained condition on the liquefaction ability of the specimen can be easily seen. Increasing the loading amplitude causes faster liquefaction of the specimen with fewer cycles, through 773 cycles with the loading amplitude of 60 kPa

and through 1738 cycles with the loading amplitude of 50 kPa. At the time of the liquefied specimen, the axial strain and damping ratio increase suddenly (Figures 10 and 11). In addition, the strength of the specimen is almost completely lost, causing specimen destruction (Figure 12). This is consistent with several findings in previous years (Vucetic & Mortezaie, 2015).

The rule of the excess pore water pressure formation, strength decline and sudden increase in damping ratio and axial strain under undrained cyclic load is also observed in the behavior of natural red sand, which has been researched and published previously by the authors. However, considering the same loading amplitude of 60 kPa and frequency of 0.5 Hz, the liquefaction ability of natural red sand is faster than that of river sand which is shown as 184 liquefaction cycles of natural red sand and 773 cycles of river sand (Van Thuy Do, Duc Tiep Pham, Van Hieu Nguyen & Cao Thang Pham, 2024). It is shown that, under undrained cyclic load, river sand has a better liquefaction resistance than natural red sand. The reason is that river sand has many rough particles which create hook insertion, forming a better connection between the particles.

The results also provide interesting data. As the load

amplitude increases, the damping ratio becomes higher in both conditions (Figures 8 & 11 and Table 2). It can be seen that there is another trend of the Young's-modulus values, which is a high value corresponding to a big amplitude in undrained condition and the opposite in drained condition (Figures 9 & 12 and Table 2).

The drained tests focused on the results of strain accumulation. Although damping ratio and strength are also considered, they increase very little (Figures 8 & 9). Further, under drained condition, the experiments allow volume changes; so, the pore water pressure does not form. Therefore, the sand specimens become more compacted and solid, but they need to be additionally examined at a higher number of loading cycles.

In two cases of load amplitude of 50 kPa and 60 kPa under undrained condition, the axial strain and damping ratio are completely consistent with the results given by Vedran Jagodnik and Željko Arbanas (2022).

Varying load magnitudes play a vital role in the operation of different loads depending on the type of construction. For example, in the foundation of traffic construction, excessive vehicle loads can cause liquefaction and destruction of the foundation if it is flooded.

CONCLUSIONS

The change in loading amplitude greatly affects the strength of the construction foundation. In case of heavy rain, it can cause flooding that completely saturates the foundation. Thence, under the effect of dynamic loads, it can cause serious consequences for the structure. The

REFERENCES

- Alotaibi, E., Omar, M., Arab, M.G., and Tahmaz, A. (2022, February). "Prediction of fine-grained soils' shrinkage limits using artificial neural networks". In: 2022 Advances in Science and Engineering Technology International Conferences (ASET), 1-5.
- Al-Sadoon, Z.A., Alotaibi, E., Omar, M., Arab, M.G., and Tahmaz, A. (2023). "AI-driven prediction of tunneling squeezing: Comparing rock-classification systems". *Geo-technical and Geological Engineering*, 1-23.
- ASTM D1557-12. (2021). "Standard test methods for laboratory compaction characteristics of soil using modified effort".
- ASTM D422-63. (2002). "Standard test method for particle-size analysis of soils".
- ASTM D698-12. (2021). "Standard test methods for laboratory compaction characteristics of soil using standard effort".
- ASTM D7181-20. (2020). "Standard test method for consolidated drained triaxial compression test for soils".
- ASTM D7263-21. (2021). "Standard test methods for laboratory determination of density and unit weight of soil specimens".
- ASTM-D3999 (2019). "Standard test methods for the behavior of sand specimens subjected to cyclic load with varying loading magnitudes under different drainage conditions in this study is important for engineers to be able to better predict the characteristics of soil in various geo-technical applications, such as foundation design, slope-stability analysis, etc.

The results show that the loading amplitude greatly influences the soil behavior and the accumulated strain under both drained and undrained conditions. Bigger loading amplitude causes higher damping ratio in both cases; however, the strength value tends to be opposite in the two cases.

The axial strain of the experimental soil shows interesting behavior under both drained and undrained conditions. Under undrained condition, the soil degrades rapidly with suddenly increasing and unrecoverable axial strain at the time of liquefied specimen. Further, the pore water pressure accumulates significantly to destroy the specimen. In drained condition, the material seems to be more compacted and solid under the effect of cyclic loads, but needs to be additionally examined at a higher number of loading cycles.

These findings are expected to enhance geo-technical engineering by improving the understanding of soil mechanics and aiding in designing safer, more effective structures.

Acknowledgements

This study was supported by the Geo-technical Laboratory at Le Quy Don Technical University, Hanoi, Vietnam. The authors are very grateful to the experts for their constructive comments.

- determination of the modulus and damping properties of soils using the cyclic triaxial apparatus”.
- Braja M. Das, and Khaled Sobhan. (2013). “Principles of geo-technical engineering”. Eighth Edition. Cengage Learning.
- BS 1377-3. (1990). “Methods of test for soils for engineering purposes. Chemical and electro-chemical tests”.
- Chengshun Xu, Chaoqun Feng, Xiuli Du, and Xiaoling Zhang. (2020). “Study on liquefaction mechanism of saturated sand considering stress redistribution”. *Engineering Geology*, 105302, <https://doi.org/10.1016/j.enggeo.2019.105302>
- Danielle Caroline Ferreira, and Façal Massad. (2022). “Evaluation of stress history and undrained shear strength of three marine clays using semi-empirical methods based on piezocone test”. *Soils and Rocks*, 1-14. DOI: 10.28927/SR.2022.075221
- Dash, H.K., and Sithara, T.G. (2016). “Effect of frequency of cyclic loading on liquefaction and dynamic properties of saturated sand”. *Int. J. Geotech. Eng.*, 1-6. DOI: 10.1080/19386362.2016.1171951
- Duque, J., Roháč, J., and Mašín, D. (2022). “On the influence of drained cyclic preloadings on the cyclic behaviour of Zbraslav sand”. *Soil Dynamics and Earthquake Engineering*, 107666. <https://doi.org/10.1016/j.soildyn.2022.107666>
- El Kahi, E., and Khouri, M. (2019). “Investigating the differences between various deterministic liquefaction correlation methods”. *Soils and Rocks*, 155-166. DOI: 10.28927/SR.422155
- Ghionna, V.N., and Porcino, D. (2006). “Liquefaction resistance of undisturbed and reconstituted specimens of a natural coarse sand from undrained cyclic triaxial test”. *J. Geotech. Geoenviron. Eng.*, 194-202. [https://doi.org/10.1061/\(ASCE\)1090-0241\(2006\)132](https://doi.org/10.1061/(ASCE)1090-0241(2006)132)
- Hou, T.S., Liu, J.L., Luo, Y.S., and Cui, Y.X. (2020). “Triaxial compression test on consolidated undrained shear-strength characteristics of fiber-reinforced soil”. *Soils and Rocks*, 43-55. DOI:10.28927/SR.431043
- Jianfeng Li, Jie Cui, Yi Shan, Yadong Li, and Bo Ju. (2020). “Dynamic shear modulus and damping ratio of sand-rubber mixtures under large strain range”. *Materials*. <https://doi.org/10.3390/ma13184017>
- Jradi, L. (2018). “Study of the influence of fine particles on the properties of liquefaction of sands”. PhD Thesis University Paris-Est. <http://pastel.archives-ouvertes.fr/tel-01970957>
- Kumar, S.S., Krishna, A.M., and Dey, A. (2017). “Evaluation of dynamic properties of sandy soil at high cyclic strains”. *Soil Dynam. Earthq. Eng.*, 157-167. <https://doi.org/10.1016/j.soildyn.2017.05.016>
- Kumruzzaman, M., and Yin, J. (2012). “Stress-strain behaviour of completely decomposed granite in both triaxial and plane strain conditions”. *Jordan Journal of Civil Engineering*, 6 (1), 83-108.
- Li, G. (2004). “Advanced soil mechanics”. TsingHua University.
- Magnos Baroni, Marcio de Souza, and Soares de Almeida. (2022). “Undrained shear-strength correlation analysis based on vane tests in the Jacarepaguá lowlands, Brazil”. *Soils and Rocks*, 1-7. DOI: 10.28927/SR.2022.072721
- Malik Belmokhtar, Pierre Delage, Siavash Ghabezloo, and Nathalie Conil. (2018). “Drained triaxial tests in low-permeability shales: Application to the Callovo-Oxfordian claystone”. *Rock Mechanics and Rock Engineering*, 1979-1993. DOI:10.1007/s00603-018-1442-0
- Md Asfaque Ansari, and Lal Bahadur Roy. (2023). “Effect of geogrid reinforcement on shear-strength characteristics of a rubber-sand mixture under undrained triaxial test”. *Jordan Journal of Civil Engineering*. DOI:10.14525/JJCE.v17i2.01
- Ni, X., Ye, B., Ye, G., and Zhang, F. (2020). “Unique determination of cyclic instability state in flow liquefaction of sand”. *Mar. Georesour. Geotechnol.*, 1-9. <https://doi.org/10.1080/1064119X.2020.1791289.0>
- Okur, D.V., and Umu, S.U. (2018). “Dynamic properties of clean sand modified with granulated rubber”. *Adv. Civ. Eng.*, 1-11. <https://doi.org/10.1155/2018/5209494>
- Omar, M., Alotaibi, E., Arab, M.G., Shanableh, A., Malkawi, D.A.H., Elmehdi, H., and Tahmaz, A. (2023). “Harnessing nature-inspired soft computing for reinforced-soil bearing-capacity prediction: A neuro-nomograph approach for efficient design”. *International Journal of Geosynthetics and Ground Engineering*, 9 (4), 53.
- Peacock, W.H., and Seed, H.B. (1968). “Sand liquefaction under cyclic-loading simple-shear conditions”. *J. Soil Mech. Found. Div.*, 689-708.
- Pingxin Xia, Longtan Shao, Wen Deng, and Chao Zeng. (2022). “Evolution prediction of hysteresis behavior of sand under cyclic loading”. *Processes*, 879. <https://doi.org/10.3390/pr10050879>
- Saud A. Sultan. (2012). “Effect of aircraft dynamic loads

- on airport asphalt pavement". Pavement Engineering and Road Materials, 2-10. <https://www.researchgate.net/publication/319087307>
- Shrigondekar, A., and Ullagaddi, P. (2021). "Ultimate load response of a square footing subjected to axial and eccentric load on geogrid-reinforced soil". Jordan Journal of Civil Engineering, 15 (1), 77-88.
- Souza Junior, P.L., Santos Junior, O.F., Fontoura, T.B., and Freitas Neto, O. (2020). "Drained and undrained behavior of an aeolian sand from Natal, Brazil". Soils and Rocks, 263-270. DOI:10.28927/SR.432263
- TCVN 4195. (2012). "Soils: Method of laboratory determination of specific weight".
- TCVN 4198. (2014). "Soils: Laboratory methods for particle-size analysis".
- TCVN 4201. (2012). "Soils: Laboratory methods for determination of compaction characteristics".
- TCVN 8721. (2012). "Soils for hydraulic engineering construction: Laboratory test method for determination of maximum and minimum dry volumetric weight of non-cohesive soil".
- Toru Shibata, Hiroshi Yukitomo, and Manabu Miyoshi. (1972). "Liquefaction process of sand during cyclic loading". Soils and Foundations, 1-16. <https://doi.org/10.3208/sandf1960.12.1>
- Van Thuy Do, Duc Tiep Pham, Van Hieu Nguyen, and Cao Thang Pham. (2024). "Influence of loading frequency and relative compaction on liquefaction behavior of reconstituted sand in cyclic triaxial tests". Rock and Soil Mechanics.
- Vedran Jagodnik, and Željko Arbanas. (2022). "Cyclic behaviour of uniform sand in drained and undrained conditions at low-confining stress in small-scale landslide model". Sustainability, 12797. <https://doi.org/10.3390/su141912797>
- Vucetic, M., and Mortezaie, A. (2015). "Cyclic secant shear modulus *versus* pore water pressure in sands at small cyclic strains". Soil Dyn. Earthq. Eng., 60-72.
- Wichtmann, T., Niemunis, A., and Triantafyllidis, Th. (2005). "Strain accumulation in sand due to cyclic loading: Drained triaxial tests". Soil Dynamics and Earthquake Engineering, 967-979. <https://doi.org/10.1016/j.soildyn.2005.02.022>
- Ye, B., Xie, X., Zhao, T., Song, S., Ma, Z., Feng, X. et al. (2020). "Centrifuge tests of macroscopic and mesoscopic investigation into effects of seismic histories on sand-liquefaction resistance". J. Earthq. Eng., 1-23. <https://doi.org/10.1080/13632469.2020.1826373.00>
- Ying Liu, Zhixuan Liang, Zhiyong Liu, and Guiping Nie. (2022). "Post-cyclic drained shear behaviour of Fujian sand under various loading conditions". Marine Science and Engineering, 1499. <https://doi.org/10.3390/jmse10101499>
- Zhang, J., Cao, J., and Huang, S. (2019). "Experimental study on the effects of initial shear stress and vibration frequency on dynamic strength of saturated sands". Ann. Mater. Sci., Eng., 1-9. <https://doi.org/10.1155/2019/3758527>
- Zhehao Zhu, Feng Zhang, Qingyun Peng, Jean-Claude Dupla, Jean Canou, Gwendal Cumunel, and Evelyne Foerster. (2021). "Effect of loading frequency on sand-liquefaction behaviour in cyclic triaxial tests". Soil Dynamics and Earthquake Engineering. 106779. <https://doi.org/10.1016/j.soildyn.2021.106779>
- Zhenzhen Nong, Sung-Sik Park, Sueng-Won Jeong, and Dong-Eun Lee. (2020). "Effect of cyclic-loading frequency on liquefaction prediction of sand. Applied Sciences, 4502, <https://doi.org/10.3390/app10134502>
- Zhu, Z., Zhang, F., Peng, Q., Chabot, B., and Dupla, J. (2021). "Development of an auto compensation system in cyclic triaxial apparatus for liquefaction analysis". Soil Dynam. Earthq. Eng., 106707, <https://doi.org/10.1016/j.soildyn.2021.106707>